# Optimizing $\sigma^0$ information from the Jason-2 altimeter

*Graham D. Quartly*

(accepted by IEEE Geoscience & Remote Sensing Letters Dec. 28th 2008)

**Abstract**

A radar altimeter's normalized backscatter, $\sigma^0$, is used in many oceanographic applications, to infer values of wind speed, wind stress, rain rate and the presence of biogenic slicks. The waveform retracker used to estimate the key geophysical variables for the altimeters on the Jason-1 and Jason-2 satellites shows increased small-scale variability since the problem is ill-conditioned. A simple empirical adjustment to $\sigma^0$ improves the separability between various parameters and also improves the along-track profiles of $\sigma^0$. This leads to i) more realistic wind fields, ii) better discrimination of rain events, and iii) improved comparison between the Jason-1 and Jason-2 altimeters during their tandem mission.

**Keywords**

altimeter, retracking, sigma0, Jason-2, data quality, reprocessing

## 1. Introduction

The radar altimeter is a nadir-pointng instrument that emits radar pulses and records their subsequent reflection from the Earth's surface. The altimeter echo from a uniform rough ocean surface has a well-defined shape (see Fig. 1) known as a Brown-like waveform [1]. The three key geophysical parameters — altimetric range (time delay), significant wave height (SWH, leading edge slope) and normalized backscatter strength (amplitude) — are readily derived by various waveform-fitting techniques [2]. The backscatter values, termed $\sigma^0$, have been used in a wide variety of applications. First of all, the backscatter is modulated by sea surface roughness on scales of a few radar wavelengths (for $K_u$-band altimeters, $\lambda$~2.3 cm); consequently $\sigma^0$ has long been used to infer wind speed, and more recently other metocean parameters, such as wave period [3].

The advent of dual-frequency altimeters (with a longer wavelength second channel, C-band for TOPEX, Jason-1 and Jason-2; S-band for Envisat) appeared to give some redundancy in wind speed information, but in fact closer analysis showed some subtle differences. In some cases, these were related to extra information about the air-sea interface e.g. wind stress [4] or presence of surface slicks [5]. In other examples, the difference in recorded $\sigma^0$ values at the two frequencies was due to attenuation by large water droplets (principally rain) within the intervening atmospheric column [6]. All such applications rely heavily on the accurate and unbiased estimate of $\sigma^0$ from waveform data.

Various techniques have been used to estimate these key geographical parameters. At the start of the Jason-1 mission, the retracker used to do this was the MLE-3, so-called as it was a Maximum Likelihood Estimator of the three variables of interest. However, problems were noted in the waveform-fitting process [7] because the spacecraft failed to keep the altimeter pointing directly to nadir leading to changes in the slope of the waveform's trailing edge (see Fig. 1). Given that the radar antenna has a beamwidth (full-width half-maximum) of typically 1.2˚, a mispointing angle, $\psi$, of say 0.3˚ can have a noticeable effect on the waveform, with the change in slope being proportional to $\psi^2$. Consequently the retracker adopted for Jason-1 and later for Jason-2 has been the MLE-4, with the 4th parameter to be estimated being $\psi^2$. When the estimated value of $\psi^2$ is positive, it represents a raising of the trailing edge slope, possibly due to off-nadir mispointing; when negative it represents a steepening of the trailing edge, which can not be interpreted as an actual physical mispointing of the instrument. However, changes in amplitude and trailing edge slope (both positive and negative) may be induced by inhomogeneities on the sea surface leading to weaker or stronger reflection at nadir than in the immediate surroundings. This may be due to rain or surface slicks, and explains why changes are observed in $\psi^2$ on much shorter scales than would be found for physical mispointing of the altimeter platform, which would tend to drift slowly. To clearly separate these two apparent causes of mispointing, I determine a 2000 km running mean of $\psi^2$, and only keep data when the modulus of this is less than 0.025 deg$^2$. This editing criterion is more important for Jason-1 (see section 3), which has a recognised problem with its attitude control.

However, as pointed out in [8], the effects of $\psi^2$ and $\sigma^0$ on the waveform shape are correlated, leading to an ill-conditioned Fisher Information Matrix, and consequently large errors for any estimation algorithm [9]. This increases the error in $\sigma^0$ due to "overfitting" of the waveform data, which manifests itself as pronounced short-scale variations in $\sigma^0$, and concomitant changes in $\psi^2$ (see Fig. 2). These effects may be particularly pronounced near rain cells, where

accurate unbiased $\sigma^0$ values are needed for dual-frequency rain-flagging [6,10,11]. The derived attenuation at $K_u$-band, $A_1$, is defined as the observed $\sigma^0_{Ku}$ minus that expected given the C-band value [6,10,11]. However, in the example illustrated (Fig. 2d), $A_1$ varies on a point-by-point basis, not consistent with real patterns of rain.

The following section shows how to make an adjustment for the MLE-4's mis-estimation of $\sigma^0$, and section 3 documents the improved geophysical estimates.

## 2. Details of $\sigma^0$ adjustment

The concept of the MLE-4 for altimetry retracking was described by Amarouche et al. [7], whose simulations suggest that values of $\psi^2$ up to 0.64 should only engender errors in $\sigma^0$ of order 0.01 dB. However, the short scale variability observed in Fig. 2a is clearly much greater. This may be due to the mismatch of real and modelled waveforms, or to other aspects of the implementation. Unfortunately such details are in proprietary documentation unavailable to the general scientific users. Thus one needs to study the bulk correlation of errors within the output data stream to characterise the needed corrections. This empirical approach also has the advantage over simulations in that it is based upon the real waveform shape (possibly including changes in antenna pattern or the intermediate frequency filter).

The profiles of $\sigma^0$ and $\psi^2$ in the top two panels of Fig. 2 suggest that, at least in this case, a simple multiple of $\psi^2$ is all that is required. However, this does start from the supposition that the measure of sea surface roughness and thus the wind field should be smooth on scales of 6 km (the separation distance of along-track points). Correlation of $\sigma^0$ and $\psi^2$ cannot be considered on a global basis, because there are genuine spatial changes in $\sigma^0$ associated with the different geographical bands of wind, whereas correlations on a small scale e.g. the length illustrated in Fig. 2 will be adversely affected by the presence of rain cells for which sharp changes in $\sigma^0$ should be expected, but are not so readily apparent.

The solution is to go to the micro-scale, looking at changes within individual 1 Hz data records, since the Jason-2 data stream has the $\sigma^0$ and $\psi^2$ estimates at 20 Hz i.e. every 280 m along track. Given that each average (20 Hz) waveform and the attendant geophysical estimates correspond to an average over a disc ~8 km in diameter, it is clear that the true areal mean surface roughness will vary little between members of this ensemble.

The 20 estimates of $\sigma^0$ and $\psi^2$ in the course of one individual second are linearly related (Fig. 3a), with a slope of $\alpha$. This slope factor is almost constant for all 1-second ocean-only records (Fig. 3b). No obvious changes in the slope can be found for either low winds (high $\sigma^0$) or rain-affected cells. This is because this measure of the correlation of errors in $\psi^2$ and $\sigma^0$ is principally a property of the 4-parameter model used to describe the waveform shape. The mean value for each pass (half-orbit of data) is 11.36 for all the times when acquisition is via the median tracker ('B' in Fig. 3c); alternative acquisition trackers lead to values differing by only ~0.5%. Whilst the difference according to acquisition mode is intriguing, it typically amounts to less than 0.01 dB. Thus, to a very good approximation, the $\sigma^0$ value corresponding to no implied mispointing ($\psi^2$=0) can be defined by:

$$\sigma^0_{adj} = \sigma^0 - \alpha \psi^2 \qquad (1)$$

where $\alpha_{Ku}$ for Jason-2 is 11.34.

A very similar analysis can be carried out for the C-band $\sigma^0$ values, resulting in a mean correlation coefficient, $\alpha_C$ of 2.01, independent of which tracker mode is being used (Fig. 2d). Note that the MLE-3 retracker is used in the ground processing of C-band, as only 3 oceanographic parameters (range, wave height and $\sigma^0$) are to be fitted, since the mispointing value is constrained to be that found for the $K_u$-band retracking (P. Thibaut, pers. comm. 2008). Consequently the 20 Hz $\sigma^0_C$ values were regressed against $K_u$-band values of $\psi^2$. The effect of genuine physical mispointing on the trailing edge slope will vary as $\psi^2 / (\Delta\theta)^2$, where $\Delta\theta$ is the antenna beamwidth. Therefore the ratio of sensitivities, $\alpha_{Ku} / \alpha_C$ (5.64) is close to the square of the ratio of frequencies ($13.6^2/5.3^2 = 6.58$), with the difference being attributable to the MLE solution using information from more than just the trailing edge.

## 3. Efficacy of $\sigma^0$ adjustment

The $\sigma^0$ values at $K_u$-band and C-band are all adjusted according to Eq. 1, using the universal values $\alpha_{Ku}$=11.34 and $\alpha_C$=2.01. The improvements for the original case study are evident in the smoother profiles in Fig. 2c (achieved without any along-track filtering) and the perceived attenuation values, $A_2$, (Fig. 2d) more closely matching with the peaks in liquid water path (LWP) from the on-board radiometer (Fig. 2e). Note the LWP profile will not reproduce the fine scale structure of the attenuation because of the radiometer's much larger footprint, which needs to be taken into account in synergistic studies of storms [12]. This global adjustment of $\sigma^0$ values affects the spectra of along-track $\sigma^0$ variations, removing the spectral plateau induced by overfitting of the waveforms (see Fig. 4). The resultant spectra

for adjusted $\sigma^0_{Ku}$ matches that for C-band, showing a fully red spectrum i.e. one dominated by changes at the larger scales. The improvement to the spectrum of $\sigma^0_C$ is minor by comparison.

These $\sigma^0$ adjustments to both $K_u$- and C-band improve the clustering of dual-frequency backscatter observations leading to reduced scatter about the mean relationship (Fig. 5). As this is the fundamental principle upon which dual-frequency rain-flagging is based [6,10,11], this immediately translates into a clearer discrimination between minor wind-related variability and more pronounced changes associated with attenuation by rain. As well as improving estimates of rain rate, this recovery of realistic rain profiles is needed for studies of length scales of rain events [13, 14].

Finally, although 20 Hz values of $\psi^2$ are not currently available for Jason-1, the adjustment process may be carried out on the 1 Hz $\sigma^0$ values from that altimeter, using the same coefficients. This is based on the assumption that the MLE-4 processor will have similar error correlations when applied to the slightly different mean waveforms from the Jason-1 altimeter. The Jason-1/2 tandem mission, with the altimeters flying the same track 54 s apart, enables us to demonstrate this. For this evaluation both altimeters must be free from genuine physical mispointing (which is why the MLE-4 processing was introduced), and that is arranged by requiring the modulus of the long-term mean (2000 km moving average) of $\psi^2$ to be no more than 0.025 deg$^2$ for both altimeters.

With this criterion implemented, we note that the two altimeters' along-track profiles of $\psi^2$ are highly correlated (Jason-2 values being 92% of Jason-1 values, $r^2$=0.72), indicating that this is not some abstract 'noise' term, but does really represent backscatter inhomogeneities at the scale of the altimeter footprint. Second, we find that adjustment of both Jason-1 and Jason-2 $\sigma^0_{Ku}$ values does lead to a closer correspondence than leaving both unadjusted (Fig. 6). The degree of scatter is reduced by a factor of three, and also the mean offset between Jason-2 and Jason-1 now varies less with $\sigma^0$. This shift in the mean relationship is because there is a greater difference between the two altimeters' records of $\psi^2$ at low winds. There is no clear improvement in $\sigma^0_C$ comparisons between the two altimeters (not shown).

**4. Summary and conclusions**

This paper advocates a very simple empirical correction to Jason-2 (and Jason-1) $\sigma^0$ values that achieves three points.

i) It removes the small-scale tracker-induced variability, leading to smooth along-track profiles of wind speed, with a simple red spectral shape.

ii) It improves the extraction of perceived backscatter in rain events, such that the altimetric detections of liquid water more closely match those locations shown by the radiometer.

iii) It improves the comparison match-ups of Jason-1 and Jason-2 1 Hz data during the tandem mission.

Provided there is no long-term mean mispointing, then the proposed adjustments will have minimal impact on wind speed comparisons with met buoys (not attempted here because of the many years of data needed), since such validation exercises typically involve along-track averages over 50 km, whereas the adjustment process only improves altimeter wind speed estimates on shorter scales. Similarly the effect of $\sigma^0$ error on the sea state bias correction will not affect altimetric height data averaged over 50 km or more. However, other geophysical retrievals based on subtle dual-frequency differences e.g. recovery of wind stress [4], detection of biogenic slicks [5] and estimates of air-sea gas transfer [15] should all also benefit from these more resilient estimates of the true surface backscatter strength.

It has been suggested that the MLE-3 processor should be used instead for Jason-2, since the spacecraft does not suffer from attitude control problems. This would require a reprocessing of all the waveform data. I recommend that it would be simpler to add a 'sigma0 (mispointing corrected)' field to the Jason-2 data stream, rather than change from the MLE-4 that might be needed at a later period in the mission. Also this paper has not sought to make any judgement on whether the range (sea surface height) information from the MLE-4 is poorer or better than that from the MLE-3. Sandwell and Smith [16] had shown that there is significant interplay between errors in the estimation of the position of the waveform leading edge and its slope, leading to a correlation between range and SWH. Their solution was to impose a correlation length on SWH variability, whereas the correction proposed here for Jason-2 involves no along-track smoothing of data.

**Acknowledgements**

Dedicated to my Dad. Thanks to Pierre Thibaut for considerable assistance in understanding the on-board and ground-based processing. Jason-2 IGDR data were obtained from the CLS FTP server, under the OSTST-approved project 'TRIDENT II'.

**References**

[1] G.S. Brown, The average impulse response of a rough surface and its applications, IEEE J. Oceanic Eng., vol. 2, 67–74, 1977.

[2] G.S. Hayne, Radar altimeter mean return waveforms from near-normal-incidence ocean surface scattering, IEEE Trans. Antennas Propag., vol. 28, 687–692, 1980.

[3] E.B.L. Mackay, C.H. Retzler, P.G. Challenor, and C.P. Gommenginger, A parametric model for ocean wave period from Ku band altimeter data, J. Geophys. Res., vol. 113, art. no. C03029, doi:10.1029/2007JC004438, 2008.

[4] T. Elfouhaily, D. Vandemark, J. Gourrion, and B. Chapron, Estimation of wind stress using dual-frequency TOPEX data, J. Geophys. Res., vol. 103 (C11), 25101-25108, 1998.

[5] J. Tournadre, B. Chapron, N. Reul, and D.C. Vandemark, A satellite altimeter model for ocean slick detection, J. Geophys. Res., vol. 111 (C4), art. no. C04004, 2004.

[6] G.D. Quartly, T.H. Guymer, and M.A. Srokosz, The effects of rain on Topex radar altimeter data J. Atmos. Oceanic Tech. vol. 13, 1209-1229, 1996.

[7] L. Amarouche, P. Thibaut, O.-Z. Zanife, J.P. Dumont, P. Vincent, and N. Steunou., Improving the Jason-1 ground tracking to better account for attitude effects, Marine Geodesy, vol. 27 (1-2), 171-197, 2004.

[8] P.G. Challenor, and M.A. Srokosz, The extraction of geophysical parameters from radar altimeter returns from a non-linear sea surface, in Mathematics in Remote Sensing (ed. S.R. Brooks), Clarendon Press, 1989.

[9] D.R. Cox, and D.V. Hinkley, Theoretical Statistics, Chapman & Hall, ISBN: 0412161605, 1974.

[10] G.D. Quartly, Sea state and rain: A second take on dual-frequency altimetry, Marine Geodesy. vol. 27 (1-2), 133-152. & 27 (3-4), 789-795, 2004.

[11] J. Tournadre, Validation of Jason and Envisat altimeter dual-frequency rain flags, Marine Geodesy. vol. 27 (1-2), 153-169, 2004.

[12] G.D. Quartly, and T.H. Guymer, Realizing Envisat's potential for rain cloud studies, Geophys. Res. Lett.. vol. 34, art. no. L09807, doi:10.1029/2006GL028996, 2007.

[13] G.D. Quartly, M.A. Srokosz, and T.H. Guymer, Global precipitation statistics from dual-frequency TOPEX altimetry, J. Geophys. Res. 104 (D24), 31489-31516, 1999.

[14] G.D. Quartly, M.A. Srokosz, and T.H. Guymer, Changes in oceanic precipitation during the 1997-98 El Niño, Geophys. Res. Lett., vol. 27, 2293-2296, 2000.

[15] N.M. Frew, D.M. Glover, E.J. Bock, and S.J. McCue, A new approach to estimation of global air-sea gas transfer velocity fields using dual-frequency altimeter backscatter, J. Geophys. Res., vol. 112 (C11), art. no. C11003, 2007.

[16] D.T. Sandwell, and W.H. F. Smith, Retracking ERS-1 altimeter waveforms for optimal gravity field recovery, Geophys. J. Int., vol. 163, 79-89, doi: 10.1111/j.1365-246X.2005.02724.x, 2005.


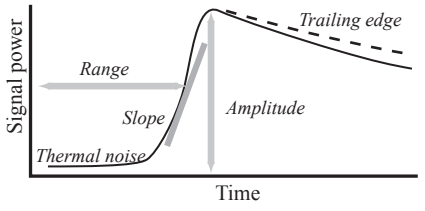


*Fig. 1 : Schematic of mean ocean waveform (thin black line). The standard oceanic parameters to be estimated are leading edge slope (related to wave height), position of mid-point of leading edge (altimetric range) and amplitude of signal ($\sigma^0$, related to wind speed). The MLE-4 processor also estimates slope of trailing edge, with gentler slope (dashed line) interpreted as positive mispointing.*

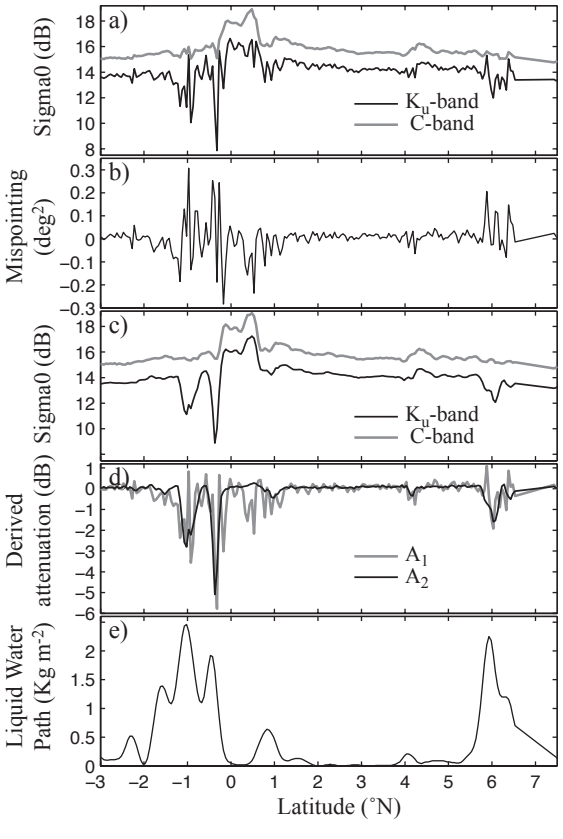


*Fig. 2 : Profiles of altimetric data along cycle 6, pass 238. a) Original $\sigma^0$ values, b) Mispointing angle, $\psi^2$, c) Adjusted $\sigma^0$ values, d) Derived attenuation values, e) Liquid water path from on-board radiometer.*

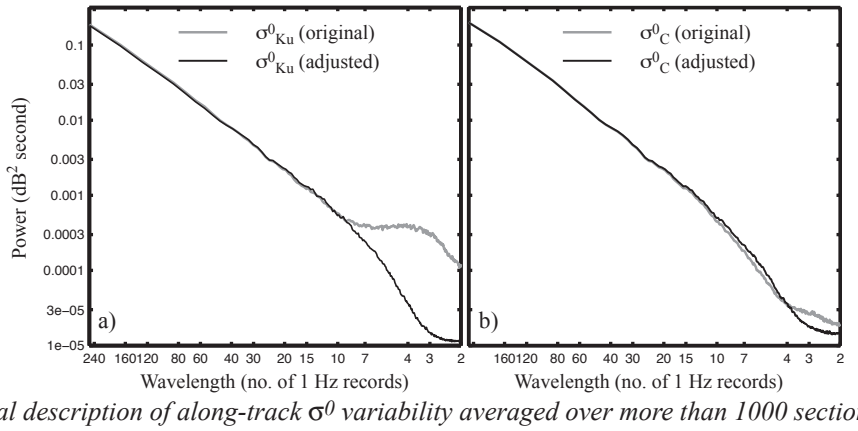


*Fig. 4 : Spectral description of along-track $\sigma^0$ variability averaged over more than 1000 sections from cycles 6-8. a) $K_u$-band, b) C-band.*

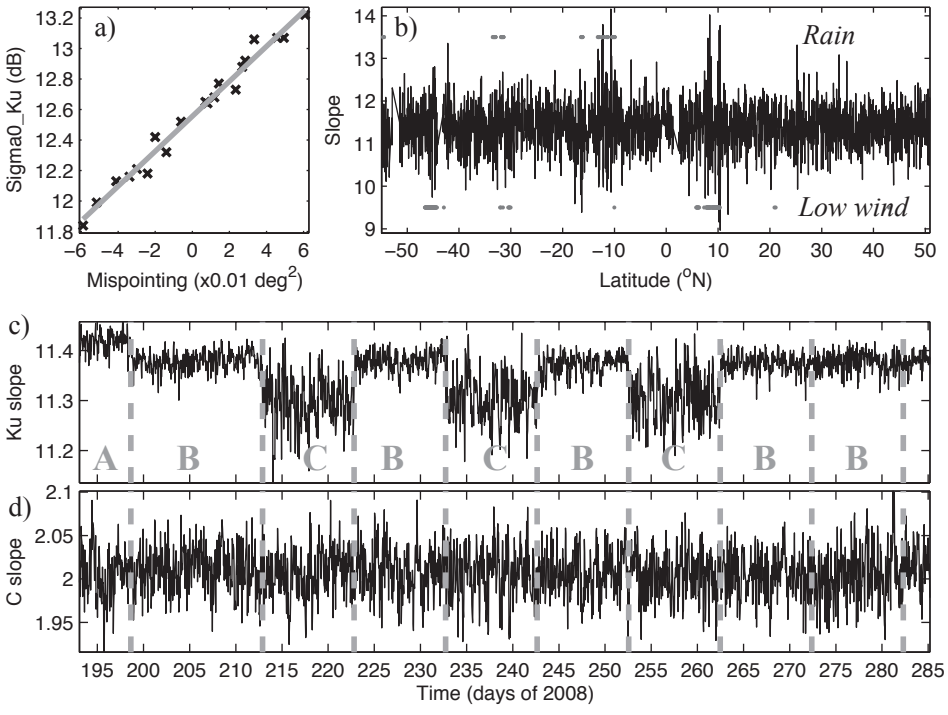


*Fig. 3 : a) Scatter plot of 20 $\psi^2$ and $\sigma^0$ values from one individual second of data. b) Derived slope for each second of oceanic data in that pass (cycle 6, pass 197). For more than 98% of points the 20 Hz $\psi^2$ estimates include positive and negative values i.e. they span $\psi^2$=0. Dots at top of plot show possible rain (LWP>0.4 kg m$^{-2}$); dots along bottom are low wind conditions ($\sigma^0_{Ku}$ >15 dB). c) Mean slope for each individual pass in the first 9.3 10-day cycles of data, d) Same for C-band. The vertical dashed lines indicate changes in the tracker controlling the acquisition of data on-board: A - split gate tracker, B - median tracker, C - DIODE coupled mode.*

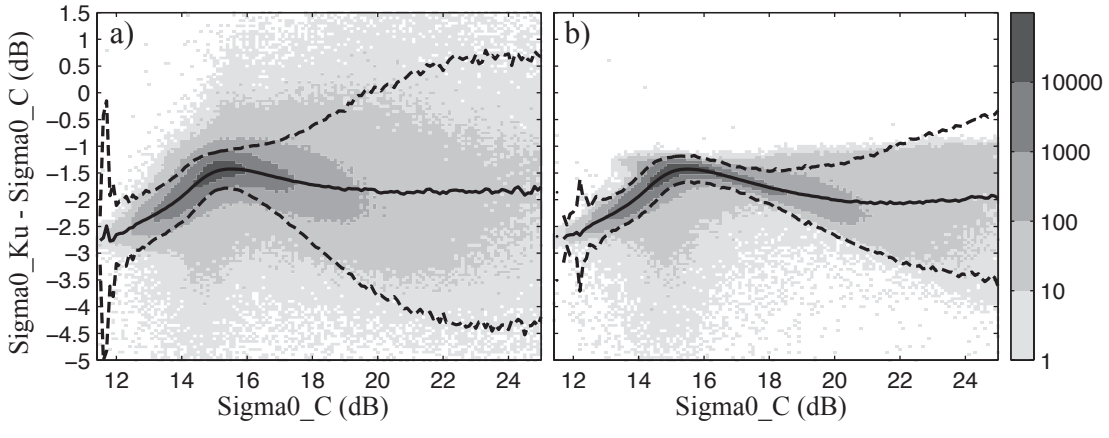


*Fig. 5 : Two-dimensional histograms of simultaneous 1 Hz $\sigma^0$ observations during Jason-2 cycles 5-14, with added lines showing mean (solid) and +/-2 std. dev (dashed) a) Original values, b) Adjusted values.*

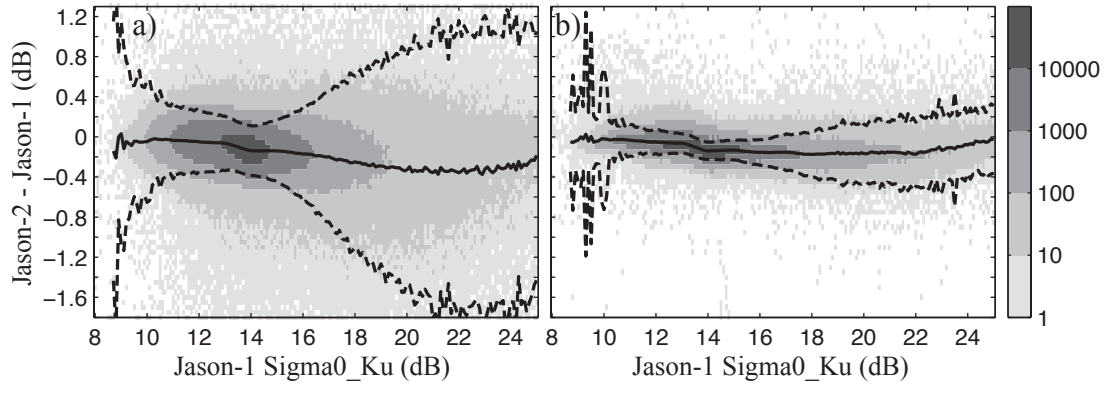


*Fig. 6 : Two-dimensional histograms of co-registered Jason-1 and Jason-2 $\sigma^0_{Ku}$ records. Data are from Jason-2 cycles 5-14 (Jason-1 cycles 244-253), with added lines showing mean (solid) and +/-2 std. dev (dashed) a) Original values, b) Adjusted values. (Jason-1 values are linearly interpolated to latitude of Jason-2 records.)*